Bioelectrorheological Model of the Cell. 5. Electrodestruction of Cellular Membrane in Alternating Electric Field

Piotr Pawłowski,* Irena Szutowicz, Piotr Marszałek,‡ and Magdalena Fikus*
*Institute of Biochemistry and Biophysics, Polish Academy of Sciences, Rakowiecka 36, 02-532 Warsaw, Poland; ‡Electrotechnical Research Institute, Pożaryskiego 28, 04-703 Warsaw, Poland

ABSTRACT Recently proposed analysis of the extensil stress developed in a cellular membrane subjected to an alternating electric field (Pawłowski, P., and M. Fikus, 1993. Bioelectrorheological model of the cell. 4. Analysis of the extensil deformation of the membrane in an alternating electric field. *Biophys. J.* 65:535–540) was applied in calculations of extensil stress threshold values, $\sigma_{0[}^{e}[d]$, producing experimentally observed electrodestruction of cells within the frequency range of $7 \times 10^1 - 3 \times 10^5$ Hz. It was shown that the susceptibility ($s[d] = 1/\sigma_{0[}^{e}[d]$), of the membrane to this process varies with field frequency and depends on the type of cells. Electrodestruction is facilitated in the 10^5-Hz field.

A rheological hypothesis explaining the experimentally observed dependence of membrane stability on electric field frequency was proposed and successfully tested for two other phenomena: electroporation and electrofusion.

INTRODUCTION

In discussions on the mechanisms leading to destabilization of the cellular membrane in an electric field, the mechanical properties of the membrane, as well as the distribution of the field of mechanical forces created by electric field are often disregarded.

Experimental studies of electrodestruction of single cells subjected to external alternating electric field within the frequency range of $f = 7 \times 10^1$–3×10^5 Hz ($f = \omega/2\pi$) were initiated in order to gain insight into the mechanical features of this process. The data were statistically evaluated, and the results were analyzed accordingly to the recently developed electromechanical model (1).

The experimental results clearly exposed the effect of field frequency on membrane stability. This phenomenon was tentatively discussed in terms of a simple rheological model of the membrane, treated as a viscoelastic body endowed with inertia. It was suggested that the contribution in energy of membrane destruction at high electric field frequencies of the heat component dominates over the respective work component.

The model was successfully applied for the description of three different phenomena resulting from the interactions of the electric field with cells of different origin: poration, fusion, and destruction. Then, the general character of the model was postulated.

This model was applied in description of the above effects and as a result rheological parameters of the system were estimated.

EXPERIMENTAL PROCEDURES

Neurospora crassa slime cells and murine myeloma (line Tib9) cells were used in the experiments.

Received for publication 23 October 1992 and in final form 11 March 1993.
Address reprint requests to Dr. M. Fikus.

0006-3495/93/07/541/09 $2.00

On the basis of theoretical analysis (1), the values of the threshold extensil stress, $\sigma_0^e[d]$, giving rise to electrodestruction of the cellular membrane, were calculated. Electrodestruction was defined as visually observed disruption of the cell. On monitor, macroscopic rupture of the membrane and release of cellular components into an external medium was observed. The width of the pulse of the alternating field giving rise to electrodestruction was 200 ms for myeloma and 2 s for the *N. crassa* cells.

In investigations of *N. crassa* cells, the approximated threshold values of voltage amplitude for electrodestruction, $V[d](f)$, were found in preliminary experiments. Then at the selected field frequency the vicinity of the estimated values ($V[d](f) \pm 30\%$) was rigorously tested using the typical step 1 V_{pp}. To decrease statistical dispersion, each experiment was repeated several times at each of the various field frequencies.

The experimental set-up and details of the procedures, as well as the physical parameters of the systems studied have previously been published for *N. crassa* (2, 3) and Tib9 (4) cells. Briefly: cells were placed in a microchamber between either two parallel platinum wire (*N. crassa* cells) or plate (Tib9 cells) electrodes to which a single pulse of alternating electric field of a given frequency within the range of $f = 7 \times 10^1$–3×10^5 Hz and of a chosen strength was applied. The range of field frequencies corresponded to the range of Maxwell-Wagner polarization in the absence of electrode polarization effects (lower limit), whereas the upper limit depended on the capacity of the generator. Since after each pulse the chamber was washed and reloaded with new cells, each cell was subjected to the electric field only once. Experiments were recorded and further analyzed on videotape, and photographs were taken for permanent records.

Analysis of the data

In the case of *N. crassa* slime cells, both positive and negative attempts at electrodestruction were taken into account in the calculations. Every investigated cell was assigned an applied maximal extensil stress value, σ_0^e, based on its individual geometric parameters and on the applied voltage (field distribution in the chamber was determined according to the "two parallel cylinders model"). Field strength, E_0, acting on the cell was estimated at a distance $+R$ from the electrode. The calculations were performed according to the electromechanical model (1) and to Appendix 2.

At a given field frequency, f = const., the set of the obtained values of the applied stress, (σ_0^e), was divided into stress magnitude intervals (i) and the probability of electrodestruction was calculated for each interval according to the formula: "$p_i[d] = n_i[d]/N_i$," where $n_i[d]$ is the number of disrupted cells and N_i is the total number of cells in the interval i. The obtained value of probability $p_i[d]$ was assigned to the upper limit of the interval, σ_{0i}^e.

Assuming that the cell is susceptible to electrodestruction if σ_0^e exceeds a certain stress which is characteristic for that cell, then the threshold value,

$p_i[d](\sigma^e_{0i})$, is equal to the probability of finding in the cell population a cell for which the threshold stress is lower than σ^e_{0i}. In this way the distribuant for the distribution of the density of probability for the threshold value of the extensil stress, giving rise to electrodestruction, was determined experimentally.

Fitting of the distribution (normal distribution was assumed) to the experimentally determined values of $p_i[d](\sigma^e_{0i})$ affords the mean value of the threshold extensil stress at electrodestruction, $\sigma^e_0[d]$, standard deviation in the population of cells, and standard errors of their determination.

The above procedure was repeated for the full spectrum of the frequencies studied. As a result a set of $\sigma^e_0[d](f)$ values was obtained. On the average the standard error of the mean values was more than 2-fold smaller than the standard deviation itself; the level of significance for the fitting procedure was acceptable ($a = 0.015$).

The data analyzed as above are helpful in establishing the characteristic property of cells, i.e., their susceptibility to electrodestruction defined as $s[d] = 1/\sigma^e_0[d]$. Errors in the determination of $s[d]$ could be found only if the complete differential method was applied to estimations of $\sigma^e_0[d](f)$ and their standard errors.

In the case of Tib9 cells only the successful attempts (i.e., those leading to electrodestruction) were taken into account. For a given field frequency, f, the amplitude of field strength $E_0[d](f)$ was averaged for the series of replicates and the mean value of the threshold mechanical extensil stress $\sigma^e_0[d](f)$ corresponding to $E_0[d](f)$ was calculated according to the electromechanical model (1) and to Appendix 2.

RESULTS

It was demonstrated and statistically confirmed that electrodestruction of *N. crassa* cells strongly depends on the electric field frequency (Fig. 1 *a*). The question of whether these findings are specific for the investigated type of cells or whether the observed relationship is of a general nature was approached in preliminary experiments with mammalian Tib9 cells (Fig. 1 *b*). The results of these experiments suggest the latter assumption is true.

It may be anticipated, however, that the susceptibility of the cellular membrane to alternating electric field should in some way depend on the type of cells. In the case of *N. crassa* and Tib9 cells this dependence manifested itself by the difference between these cells in pulse width giving rise to a similar membrane response under otherwise analogous conditions (Fig. 1).

With a rise of the electric field frequency the susceptibility of cells to electrodestruction increased to relatively high values (at $f \simeq 10^5$ Hz). Fig. 1 points to the occurrence of a transient decrease in susceptibility to destruction, $s[d]$, between its low-frequency plateau and the abruptly rising part of the curve at high frequencies; this was quantitatively confirmed for *N. crassa* cells.

DISCUSSION

In a recently proposed theoretical analysis (1) the periodic stress developed in the cellular membrane in alternating electric field has been averaged over the field period, which means that the corresponding periodic deformations were averaged as well. The experimental results clearly indicated that the observed phenomena are frequency dependent. Thus constant values for the averaged extensil stress, obtained on the assumption of the frequency dependence of Maxwell-

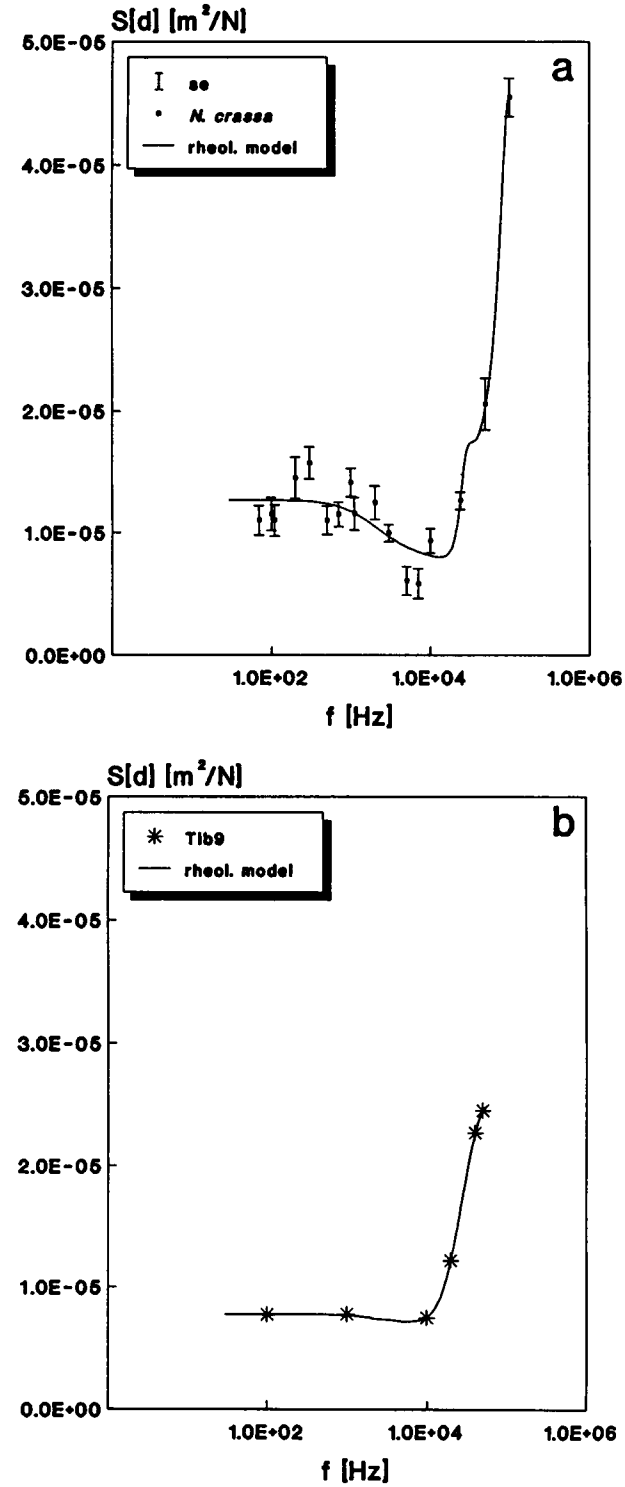

FIGURE 1 Electrodestruction of *N. crassa* (*a*) and Tib9 (*b*) cells subjected to pulses of an alternating electric field of various amplitudes and frequencies, and with fixed width (2 s and 200 ms, respectively). Conductivities of the external medium: $\mathrm{Re}[\hat{k}] = 12$ and 2 mS/m, respectively. Electric and geometric parameters as reported previously (2–4, 12) and as in Appendix 2. Susceptibilities of the membrane to electrodestruction, $s[d]$, were calculated according to Appendices 1 and 2 of Ref. 1. Vertical bars denote the errors calculated using the complete differential method based on standard errors for the mean values, (see Results). *N. crassa* (436) and Tib9 (30) cells (*a* and *b*, respectively) were measured in separate experiments. Solid line represents predictions derived from the rheological model (Appendix 1).

Wagner polarization, cannot be accepted as specific for the observed effects. Let us consider the possible causes of this dependence.

When acting on constituents of the membrane endowed with electric charges, electric field induces an additional membrane potential; its value depends on field frequency (4). The induced membrane potential was therefore estimated. At low field frequencies it attained the level of 550–650 mV, which exceeded the resting membrane potential by more than 2-fold. Similarly, as for most mammalian cells, the resting potential is probably close to 100 mV for Tib9 and was determined as 200 mV for *N. crassa* cells (5). Therefore it could be anticipated that the stress created by Maxwell-Wagner polarization would exceed by more than 2-fold the stress created by the interactions between external electric field and primary charges located in the cellular membrane. The induced potential dropped with an increase in field frequency (4), whereas the susceptibility of the membrane to stress rose. These are the arguments testifying against the important role of the induced membrane potential for the susceptibility of the membrane to destabilization by electric field, as a function of field frequency.

The entirely elastic character of the membrane has previously been assumed, when its deformation was analyzed (1). The starting assumption was that the variations of membrane area and thickness, averaged over time, are the specific invariable parameters responsible for disturbance in membrane integrity (at a constant coefficient of biaxial elasticity). As shown by the present experiments, this may be true only at low field frequencies, when compliance of the membrane to destabilization by electric field is constant.

When field frequency increased, together with a corresponding rise of the frequency of extensil mechanical oscillations, there was need (revealed and confirmed by experimental results) to consider the oscillatory character of stress, and to take into account viscous dissipation of energy, consistently with the rheological model of the membrane subjected to extensil deformation.

The simple model of a viscoelastic body with mass, exposed to oscillatory stress (Fig. 2), allows for variations of both the viscosity and elasticity parameters. It was assumed

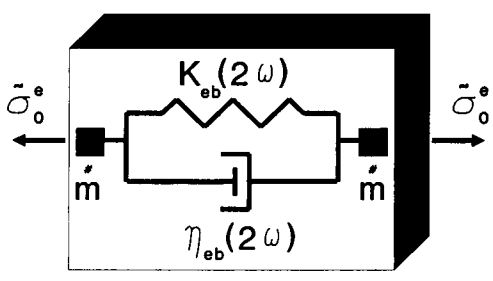

FIGURE 2 Rheological model of a cellular membrane subjected to extensil stress: $\bar{\sigma}^e_0$ is the periodic extensil stress within the membrane, $K_{eb}(2\omega)$ is the area elastic modulus of the membrane, $\eta_{eb}(2\omega)$ is the coefficient of viscosity, $\overset{\bullet\bullet}{m}$ is the inertia coefficient, detailed description of the model in Appendix 1.

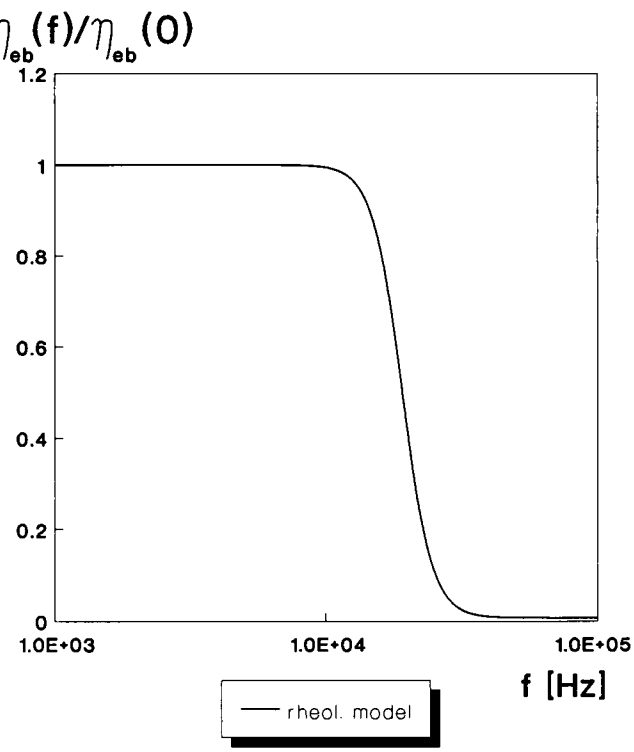

FIGURE 3 Viscosity coefficient of the membrane as a function of electric field frequency, calculated as a fitting parameter of the rheological model fitted to experimental results on electrodestruction of *N. crassa* cells (Fig. 1 and Table 1). Note that the electric field frequency amounts to a half of the corresponding frequency of mechanical oscillations.

that electrodestruction occurs when the sum of density of isothermal work performed against intermolecular forces plus the fraction of heat supplied to the membrane (and modifying these interactions) attains some threshold value. The phenomenological coefficient of combination, α, (see Appendix 1) describes the unknown part of heat essential in destabilization processes.

Analytical description of the rheological model is presented in Appendix 1; fitting of the model to the experimental results is shown in Fig. 1, *a* and *b*. At a reasonable level of significance this model could not be discarded as describing the presented data.

In accordance with the experimental results, the model permitted neglecting the specific role of field oscillations only for mechanical oscillations generated at low field frequencies, $f \leq 10^3$ Hz. Within this frequency range the function representing the analytical extension of the model remained constant.

A further increase in the frequency (10^3-10^4 Hz) was accompanied by viscous dumping of deformation. Within the frequency range $f = 10^4$-10^5 Hz the rheological model postulated, however, a sigmoidal decrease in the viscosity of structures reactive to the frequency of stress oscillations (Fig. 3). As a results of both these phenomena (viscous dumping and reduction of viscosity) the membrane susceptibility to destruction was transiently dropped and subsequently increased.

TABLE 1 Physical parameters of the electrodestruction process, obtained by fitting the rheological model (Appendix 1) to the experimental results for Tib9 and *N. crassa* cells

Cells	Tib9	*N. crassa*
$\mathrm{Re}[\tilde{k}]$(S/m)	0.002	0.012
$\Delta\tilde{S}^{max}[d]$/S	$(2.5 \pm 0.5)E-2$*	$(2.5 \pm 0.5)E-2$
$e'[d]$ (J/m^3)	$(3.2 \pm 0.8)E+3$	$(2.0 \pm 0.8)E+3$
$K_{eb}(0)$ (N/m^2)	$(1.03 \pm 0.22)E+7$	$(6.3 \pm 1.7)E+6$
$\eta_{eb}(0)$ (Ns/m^2)	$(6 \pm 3)E+2$	$(3.5 \pm 2.6)E+2$
$\eta_{eb}(\infty)$ (Ns/m^2)	$(2.8 \pm 1.8)E+1$	3 ± 3
τ(s)	$(5.77 \pm 0.27)E-6$	$(4.2 \pm 0.4)E-6$
χ'(s)	$(1.1 \pm 0.4)E-4$	$(1.7 \pm 0.9)E-4$
$\tilde{m}$ (kg/m)	$(2.6 \pm 0.6)E-5$	$(8.6 \pm 1.1)E-6$
f_r (Hz)	$5.00E+4$	$1.00E+5$
n	2	4

* E, xxx.

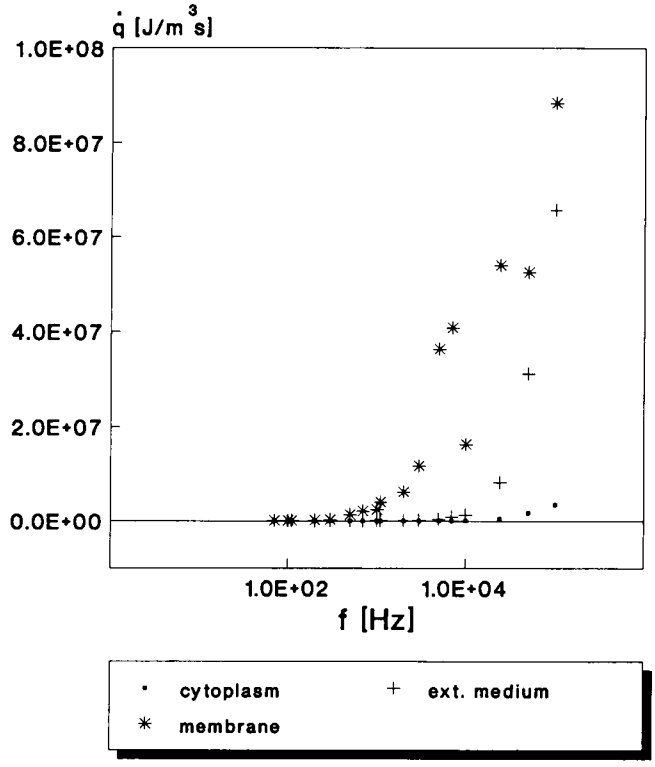

FIGURE 4 Densities of thermal efficiency of extensil oscillations, $\dot{q}^e$, and of Joule heat in the membrane, cytoplasm and external medium (close to the cell's pole), calculated after fitting the rheological model to the experimental results obtained for electrodestruction of *N. crassa* cells. Physical parameters of the process are presented in Table 1 and Appendix 2. In calculations of the Joule heat values at a given frequency, the mean value of the applied electric field amplitude was used.

At frequencies higher than $f = 10^4$ Hz a steep increase in this susceptibility occurred. It could be tentatively explained as resulting from resonance oscillations of the susceptible structures and from accompanying increase in heat supplied to the system.

It is noteworthy that the fitting parameters of the model represent in fact the rheological parameters of the membrane subjected to extensil periodic deformations (Table 1).

The frequency dependence of cell behavior could be discussed also in terms of electric currents and of resulting Joule

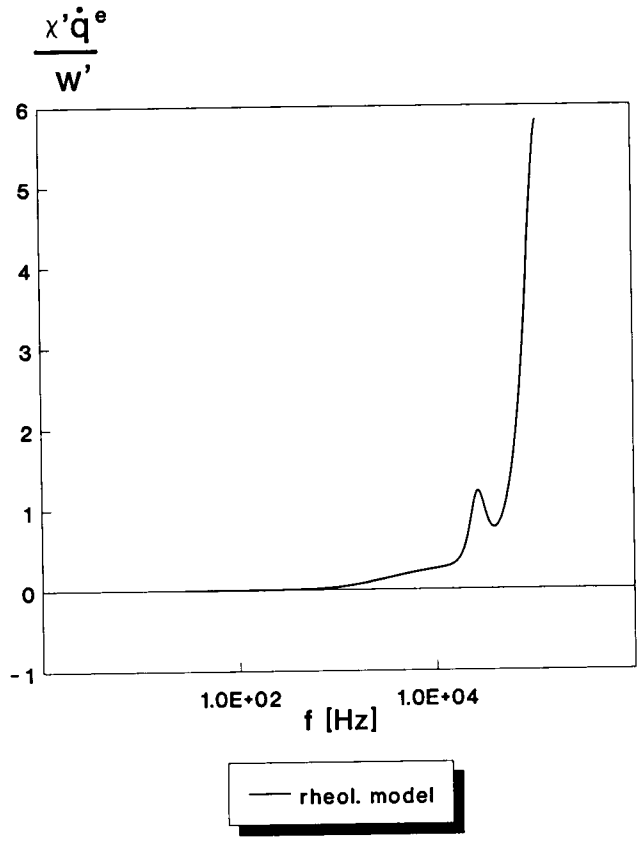

FIGURE 5 Ratio of the heat density component to the work density component of forced oscillations, calculated for the cell's pole as a function of electric field frequency. Calculations were based on fitting of the rheological model to the experimental results obtained for electrodestruction of *N. crassa* cells. Physical parameters taken from Table 1.

heat. When the rheological (Table 1) and electrical (Appendix 2) parameters of *N. crassa* were included in the calculations, it was found that the density of heat power in the membrane much more exceeds Joule power in cytoplasm than in the external medium (Fig. 4). Joule's heat in the external medium may impede heat outflow from membrane to the environment. It is difficult to predict from our model whether heat outflows from the membrane to the cytoplasm, because viscosity of the latter was not considered in this model. Furthermore, Joule heat is amplified in the vicinity of pore openings, possibly influencing the mechanical susceptibility of membranes. These effects should be closely reconsidered in a future extension of modeling of this system.

Within the range of high frequencies the contribution of heat energy prevailed over that of work performed (see Appendix 1, Eq. A23). This means that under these conditions heat energy was mainly responsible for destabilization of the membrane (Fig. 5).

It is generally accepted that electroporation also results from membrane destabilization. The mechanical factors accompanying electroporation of cellular membranes in periodic electric field have, however, been only rarely discussed and were never analytically described. In this work we applied a recently developed electromechanical model of cel-

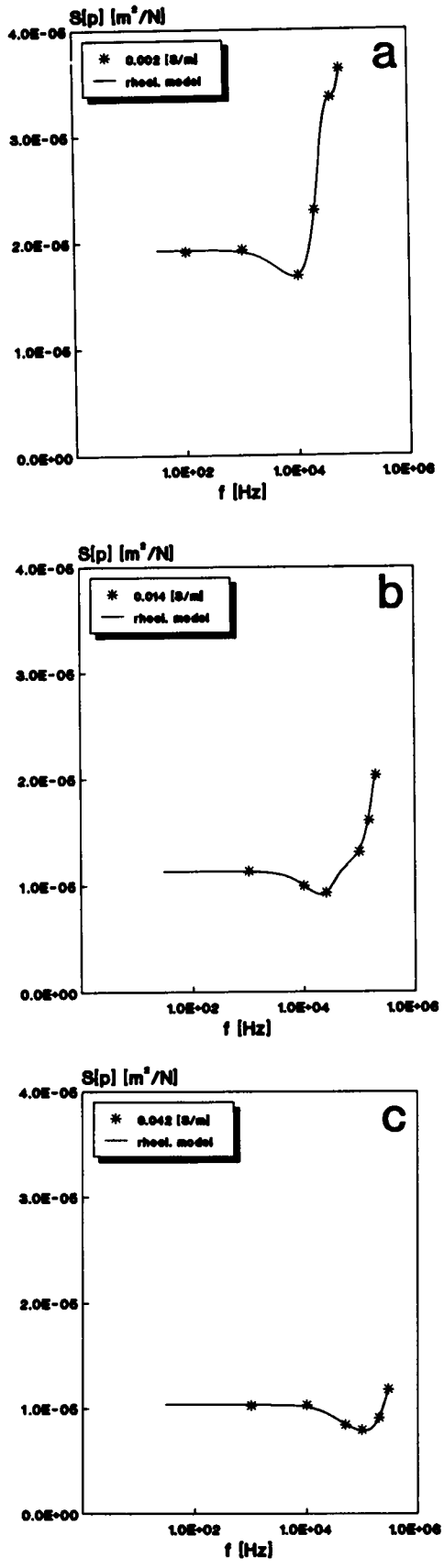

FIGURE 6 Electroporation of Tib9 cells after application of a 200-ms pulse of various amplitudes and frequencies and at various conductivities of the external medium as indicated. Each point represents the mean value of two to five replications. Experimental data reported in Ref. 4 were recalculated in terms of the cellular susceptibility to electroporation according to Ref. 1. The electric and geometric parameters used in the calculations were taken from Appendix 2. Solid line represents predictions derived from the rheological model described in Appendix 1.

lular membrane (1), exposed to alternating electric field, to the recently published results on electroporation of Tib9 cells (4). In the present studies extensil stress leading to electroporation, $\sigma_{0L}^{e}[p]$, was calculated and expressed as membrane susceptibility to poration, $s[p] = 1/\sigma_{0}^{e}[p]$. It was shown (Fig. 6) that these data could be surprisingly well expressed in terms of the proposed rheological model (Appendix 1).

The ionic strength of the external medium was found to influence the mechanical susceptibility of Tib9 cells to electroporation.

Under the same experimental conditions, the ratio of the values of Tib9 cell susceptibilities to electroporation to those to destruction remained constant only for low field frequencies, showing an abrupt decrease at higher frequencies (Fig. 7). This may imply that both processes are due to different mechanisms or/and involve different molecular structures.

Thermal chaotic motion may promote mixing of membrane molecules of two neighboring cells remaining at a short distance; this could influence their electrofusion as well. This hypothesis was checked by fitting the proposed rheological model to recently published experimental data on electrofusion of human erythrocytes (red blood cells) (RBC) (6). It was assumed that the yield of electrofusion, *efe*, is proportional to the increase above the certain threshold value in energy of intermolecular interactions responsible for the integrity of the membrane. It was also assumed that the heat energy supplied to the system considerably exceeds the difference between the isothermal work performed and the threshold energy (Fig. 8).

The successful analytical description of three different effects by one analytical model testifies to the important role of the mechanical aspects in the description of these phenomena. However, the problem of the common molecular background and temporal sequel of these effects remained unclear.

The results presented in Fig. 1 *a* point to high dispersion of the stability values of *N. crassa* cellular membranes. The dispersion of the stability data estimated on the basis of standard deviation for the population was calculated to be 2-fold higher, than that presented in the figure, based on standard error calculations. This dispersion may be attributed to different physiological states of the cells and to various moments in the cell cycle at the time of the measurements, as we have recently assumed when analyzing shear deformation of these cells (7).

The rheological model is simple yet universal since it could be used to describe of three different phenomena observed for three different cell types. Its application permitted calculation of the volumetric rheological parameters of cellular membranes (Tables 1–3). Determination of these pa-

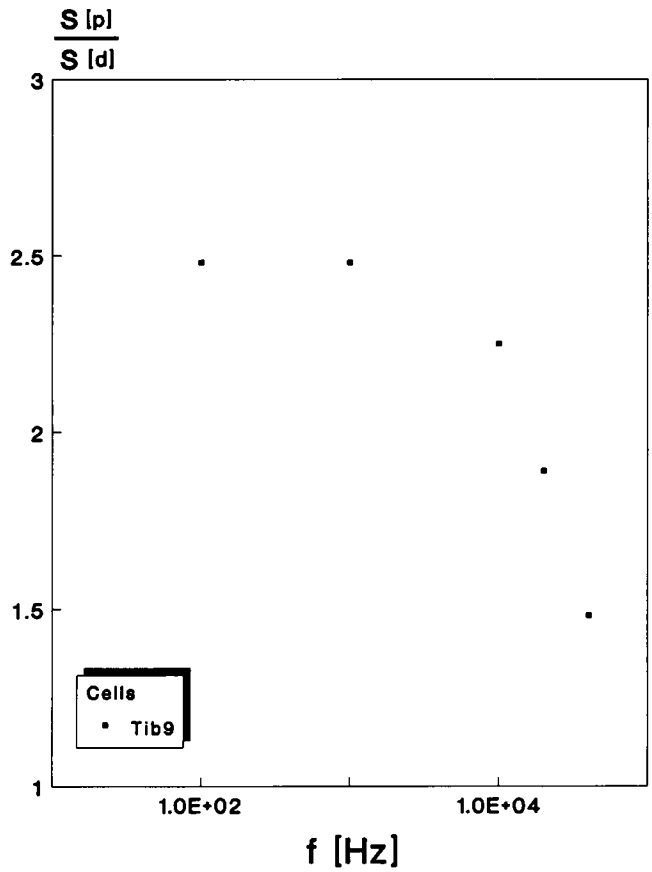

FIGURE 7 Ratio of the susceptibilities to electroporation and electrodestruction determined for Tib9 cells under the same experimental conditions. Data taken from Figs. 1 and 6 at external medium conductivity Re[$\dot{k}$] = 2 mS/m.

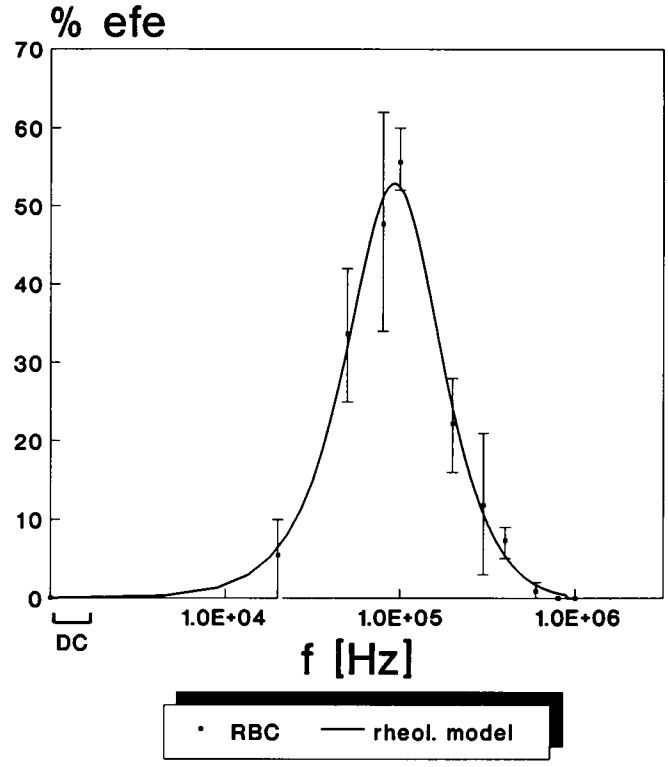

FIGURE 8 Fitting of the rheological model of the membrane (Appendix 1) to the experimental results obtained for electrofusion of human erythrocytes, where *efe* is the electrofusion yield. Fitting parameters are recorded in Table 3. Experimental results taken from Ref. 6.

rameters by other experimental methods is difficult and in some instances has never been attempted. This work demonstrates the first application of a periodic electric field for such purposes.

The values of the estimated parameters should be considered reliable only in terms of orders of magnitude, and not as precise numbers. They appear to be within the expected ranges.

The values of the rescaled coefficients of inertia, $\hat{m} \times d$ ($d = 9 \times 10^{-9}[m]$), remained within the limit values roughly estimated for membrane mass and whole cell mass, respectively: $3 \times 10^{-14} \div 1 \times 10^{-11}$ [kg] (*N. crassa*), $5 \times 10^{-15} \div 1 \times 10^{-12}$ [kg] (Tib9), and $2 \times 10^{-15} \div 3 \times 10^{-13}$ [kg] (RBC). This may suggest that some intracellular components may contribute to membrane inertia.

The values estimated for area elastic moduli remained within the range of those obtained for lipid bilayers (8) and plant protoplasts (9). When calculated for the experiments on poration, these values increased with a rise of external conductivity.

The estimated coefficients of viscosity, η_{eb} (0), have been reported to be larger than those obtained for lipid membranes (10). This testifies to the influence of membrane proteins and of the cytoskeletal network on the effective values of viscosities, determined in this work.

The values of density of the energy expended for electroporation and destruction were calculated from eq. A14, assuming that initial tension, γ_{init}, counterbalances initial surface pressure, π_{init}, and that π_{init} equals K_{eb} (0). This energy estimated for various investigated cells was found to be within the range of $(1.6 \div 2.6) \times 10^5$ (J/m^3) (Table 4). If the lipid bilayer is considered as an example, and when assuming the mean volume of lipid molecule to be $V_1 = 3 \times 10^{-27}$ (m^3), this energy corresponds roughly to 100 cal/mol. If these estimations are within the correct range this would mean that the destabilizing effects are related to the breakage of weak intermolecular interactions rather than of chemical bonds.

The energy needed for destruction of Tib9 cells is higher than that necessary for their poration; the latter increases with a rise of external medium conductivity.

The values of χ' estimated according to eqs. A11, A23, may be reasonable when assuming $\chi \cong t$ and $1/\alpha \sim 100$ (close to the number of degrees of freedom for one lipid molecule). This suggests that the exchange of heat between membrane and environment is rather slow and also that motion of small molecules is more essential in destabilization of the membrane than are their internal vibrations.

When the magnitude of errors was taken into account, it became obvious that it is impossible to indicate which of the determined parameters may be used as a distinctive

TABLE 2 Physical parameters of the electroporation process, obtained by fitting the rheological model (Appendix 1) to the experimental results for Tib9 cells

$\mathrm{Re}[\hat{k}]$ (S/m)	0.002	0.014	0.042
$\Delta\tilde{S}^{max}[p]/S$	(2.5 ± 0.6)E − 3	(8.0 ± 1.8)E − 4	(2.5 ± 0.6)E − 4
$e'[p]$ (J/m^3)	(1.3 ± 0.3)E + 2	(7.1 ± 1.6)E + 1	(2.4 ± 0.6)E + 1
$K_{eb}(0)$ (N/m^2)	(4.1 ± 0.9)E + 7	(2.2 ± 0.5)E + 8	(7.8 ± 1.7)E + 8
$\eta_{eb}(0)$ (Ns/m^2)	(1.1 ± 0.3)E + 3	(1.6 ± 0.4)E + 3	(2.3 ± 1.6)E + 3
$\eta_{eb}(\infty)$ (Ns/m^2)	(8 ± 6)E − 1	(4.6 ± 1.1)E + 1	(2.3 ± 2.6)E + 2
τ(s)	(4.96 ± 0.14)E − 6	(2.891 ± 0.021)E − 6	(4.6 ± 0.8)E − 7
χ'(s)	(3.57 ± 0.14)E − 5	(1.461 ± 0.019)E − 6	(1.8 ± 2.1)E − 6
$\overset{\bullet\bullet}{m}$ (kg/m)	(2.6 ± 0.6)E − 5	(2.6 ± 0.6)E − 5	(2.6 ± 0.6)E − 5
f_r (Hz)	1.00E + 5	2.31E + 5	4.35E + 5
n	2	2	2

TABLE 3 Physical parameters of the human erythrocyte electrofusion process, obtained by fitting the rheological model (Appendix 1) to the experimental results taken from Ref. 6.

$\mathrm{Re}[\hat{k}]$ (s/m)	0.02
$e[f]$ (J/m^3)	(2.2 ± 0.4)E + 4
$K_{eb}(0)$ (N/m^2)	(4.5 ± 1.4)E + 7
$\eta_{eb}(0)$ (Ns/m^2)	(6.2 ± 2.4)E + 1
χ (s)	3.0E − 4
$\overset{\bullet\bullet}{m}$ (kg/m)	(3.2 ± 1.2)E − 5
f_r (Hz)	(9.44 ± 0.29)E + 4
α	1.0E − 2

TABLE 4 Threshold energy of electroporation and electrodestruction of different cells at various conductivities of the external medium

	$\mathrm{Re}[\hat{k}]$ (S/m)	$e[p]$ (J/m^3)	$e[d]$ (J/m^3)
N. crassa	0.012		(1.6 ± 0.7)E + 5
Tib9	0.002		(2.6 ± 1.1)E + 5
Tib9	0.002	(1.0 ± 0.5)E + 5	
Tib9	0.014	(1.8 ± 0.8)E + 5	
Tib9	0.042	(1.9 ± 0.9)E + 5	

marker for different processes in various experiments. Tentatively, such a role may be played by χ' for the processes of destruction, and by $\Delta\tilde{S}^{max}/S$ in the case of poration.

When enriched in Fourier analysis, this model may be applied for the description of experiments performed in a periodic electric field of different temporal nature. This model complements our earlier experimental and theoretical investigations of the rheological behavior of cells exposed to different kinds of stress (7, 11, 12).

APPENDIX 1

Rheological model of the membrane

The following analysis was performed for points situated at cell poles, (θ = 0°, 180°). Oscillations in fixed state were considered.

Periodic stress, $\tilde{\sigma}_0^e$ is formulated as:

$$\tilde{\sigma}_0^e = \sigma_0^e + \mathrm{Re}[A_\sigma \exp(i_u 2\omega t)] \tag{A1}$$

where σ_0^e is the temporarily averaged extensil stress, and A_σ is the complex amplitude of extensil stress oscillations.

This equation represents a superposition of the temporarily averaged extensil stress, σ_0^e (1), and of the oscillatory component. Factor "2" related to angular frequency, ω, denotes that the mechanical stress oscillates with a frequency doubled in relation to electric field frequency (Maxwell stress is proportional to squared field frequency).

By analogy, periodic extensil oscillations, $\Delta\tilde{S}/S$, are formulated as:

$$\frac{\Delta\tilde{S}}{S} = \frac{\Delta S}{S} + \mathrm{Re}[A_S \exp(i_u 2\omega t)] \tag{A2}$$

where $\Delta S/S$ is the temporarily averaged deformation of membrane area, and A_S is the complex amplitude of oscillations of membrane area deformation.

Upon accepting the rheological model depicted in Fig. 2 (see text), and when the thermal expansion term is neglected, the constitutive equations may be formulated as:

$$K_{eb}(0)\frac{\Delta S}{S} = \sigma_0^e \tag{A3}$$

$$\overset{\bullet\bullet}{m}\frac{d^2}{dt^2}\mathrm{Re}[A_S \exp(i_u 2\omega t)]$$

$$= \mathrm{Re}[A_\sigma \exp(i_u 2\omega t)] - K_{eb}(2\omega)\mathrm{Re}[A_S \exp(i_u 2\omega t)]$$

$$- \eta_{eb}(2\omega)\frac{d}{dt}\mathrm{Re}[A_S \exp(i_u 2\omega t)] \tag{A4}$$

where $K_{eb}(2\omega)$, $\eta_{eb}(2\omega)$ are the real parts of complex elastic modulus and modulus of viscosity of the membrane, respectively, $\overset{\bullet\bullet}{m}$ (kg/m) is a measure of membrane inertia. Generally, parameters $K_{eb}(2\omega)$, $\eta_{eb}(2\omega)$, and $\overset{\bullet\bullet}{m}$ can be influenced by cytoplasm and cytoskeletal interactions and as such should be considered to be effective parameters of the membrane.

When solved, the above equations give:

$$\frac{\Delta S}{S} = \frac{1}{K_{eb}(0)}\sigma_0^e \tag{A5}$$

$$A_S = \frac{A_\sigma}{K_{eb}(2\omega) - 4\overset{\bullet\bullet}{m}\omega^2 + 2\omega i_u \eta_{eb}(2\omega)}. \tag{A6}$$

Density of mechanical power applied to the membrane through work of extensil stresses, averaged over field oscillations, equals:

$$\dot{q}^e = \frac{2\omega^2 \eta_{eb}(2\omega)\,|A_\sigma|^2}{[K_{eb}(2\omega) - 4\overset{\bullet\bullet}{m}\omega^2]^2 + [2\omega\eta_{eb}(2\omega)]^2}. \tag{A7}$$

It is also equal to the mean rate of energy dissipation in a membrane volume unit.

It is assumed that the disruptive effects in the membrane are related to the increase in the energy of intermolecular interactions responsible for the integrity of the membrane (mainly in the interfacial regions of the membrane). Such an increase may be considered to result partially from isothermal area expansion work performed against the intermolecular forces. In reality, the fraction of heat supplied to the membrane and accumulated as the thermal chaotic motion of molecules, treated as a whole (thermal oscillations, thermal expansion), may influence the energy of molecular interactions. This fraction of heat is referred to as intrinsic. The model describes nonisothermal processes when the value of intrinsic heat is included into considerations.

Density of isothermal work, w^{max}, done against the intermolecular forces, leading to maximal membrane deformation in a fixed state

$$\frac{\Delta\tilde{S}^{max}}{S} = \frac{\Delta S}{S} + |A_S| \tag{A8}$$

equals

$$w^{max} = \gamma_{init}\frac{\Delta\tilde{S}^{max}}{S} \tag{A9}$$

where γ_{init} is initial tension in the membrane (in the absence of external electric field). Here, the thermal expansion therm is omitted.

Owing to the dissipative effects and to heat exchange with the environment, the mean density of heat, q, supplied to the membrane equals:

$$q = \chi\dot{q}^e \tag{A10}$$

where χ is expressed in time units, and

$$\chi = \frac{1}{\nu}(1 - e^{-\nu t}) \tag{A11}$$

and where ν ([1/s]), is heat exchange rate, and t is the time of action of the external electric field.

Membrane stability is discussed in terms of isothermal work done against the intermolecular forces and in terms of the heat fraction used for essential modifications of the membrane energetic structure. It is postulated that the integrity of the membrane is disturbed when the sum of these energies reaches a critical threshold value, e:

$$e = w^{max} + \alpha q \tag{A12}$$

where α is heat fraction essential in distortion processes. Here, the therm of αq includes the variation in energy of thermal oscillations and the work of thermal expansion as well.

Thus, membrane integrity is disturbed when:

$$e = \gamma_{init}\frac{\Delta\tilde{S}^{max}}{S} + \alpha\chi\dot{q}^e \tag{A13}$$

and the maximal value of the relative variations of membrane surface in the absence of heat production:

$$\frac{\Delta\tilde{S}^{max}}{S} = \frac{e}{\gamma_{init}} \tag{A14}$$

Equation A13 was used in the analysis of the experiments on electroporation and electrodestruction.

When the relative shift of the electric field on both the membrane-cytoplasm and membrane-external medium boundaries is neglected, it could be assumed that:

$$|A_\sigma| = \sigma_0^e. \tag{A15}$$

The hypothetical dependence of $K_{eb}(2\omega)$ and $\eta_{eb}(2\omega)$ on frequency was expressed, respectively, by:

$$K_{eb}(2\omega) = \frac{K_{eb}(0) + K_{eb}(\infty)(2\omega\tau)^{2n}}{1 + (2\omega\tau)^{2n}} \tag{A16}$$

$$\eta_{eb}(2\omega) = \frac{\eta_{eb}(0) + \eta_{eb}(\infty)(2\omega\tau)^{2n}}{1 + (2\omega\tau)^{2n}} \tag{A17}$$

where τ is relaxation time, and n is natural power.

Electroporation and electrodestruction

It is assumed that the cell undergoes electroporation [p] or electrodestruction [d] when the summarized density of isothermal work performed against the intermolecular forces and of intrinsic heat, reaches the critical value, e[·],

$$e[\cdot] = \gamma_{init}\frac{\Delta\tilde{S}^{max}}{S} + \alpha\chi\dot{q}^e \tag{A18}$$

This equation may be transformed:

$$e'[\cdot] = \frac{K_{eb}(0)}{2}\left[\frac{\Delta\tilde{S}^{max}}{S}\right]^2 + 2\chi'\dot{q}^e\left[1 - \frac{1}{2}\frac{\alpha\chi\dot{q}^e}{e[\cdot]}\right] \tag{A19}$$

where

$$e'[\cdot] = \frac{K_{eb}(0)}{2}\left[\frac{\Delta\tilde{S}^{max}}{S}[\cdot]\right]^2 \tag{A20}$$

and

$$\chi' = \frac{e'[\cdot]}{e[\cdot]}\alpha\chi \tag{A21}$$

Owing to the approximation:

$$2\chi'\dot{q}^e\left[1 - \frac{1}{2}\frac{\alpha\chi\dot{q}^e}{e[\cdot]}\right] \cong \chi'\dot{q}^e \tag{A22}$$

of the parabolic term comprising $\dot{q}^e$ in Eq. A19 by linear function close to the ideal one for border regions of the physically important range of heat values ($0 < \alpha\chi\dot{q}^e/e[\cdot] < 1$), Eq. A19 may with some approximation be formulated:

$$e'[\cdot] = w' + \chi'\dot{q}^e \tag{A23}$$

where

$$w' = \frac{K_{eb}(0)}{2}\left[\frac{\Delta\tilde{S}^{max}}{S}\right]^2. \tag{A24}$$

Note that w' is considered as properly describing isothermic work only when the work of initial stress may be neglected (see Ref. 8).

When the system parameters are fixed, equation A23 permits estimation of the threshold stress, $\sigma_0^e[\cdot]$. Upon use of Eq. A5–A8, A15, A23, and A24, membrane susceptibility to poration or destruction, $s[\cdot] = 1/\sigma_0^e[\cdot]$, was expressed as follows.

$$s[\cdot] = \left\{\frac{1}{e'[\cdot]}\left[\frac{2\omega^2\eta_{eb}(2\omega)\chi'}{[K_{eb}(2\omega) - 4\overset{\#}{m}\omega^2]^2 + [2\omega\eta_{eb}(2\omega)]^2} + \frac{1}{2}K_{eb}(0)\right.\right. \tag{A25}$$

$$\left.\left. \times\left(\frac{1}{\{[K_{eb}(2\omega) - 4\overset{\#}{m}\omega^2]^2 + [2\omega\eta_{eb}(2\omega)]^2\}^{1/2}} + \frac{1}{K_{eb}(0)}\right)^2\right]\right\}^{1/2}$$

Theoretical predictions (Eqs. A16, A17, and A25) were fitted to the experimental results (Figs. 1 and 6, see Results). Computer simulations

showed that, within the analyzed frequency range, the variations of elasticity are negligible, resonance frequency, $f_r = 1/4\pi(K_{eb}(0)/\overset{\#}{m})^{1/2}$, is stable, and the "$n$" parameter changes within the narrow range of $2 \div 4$. In order to diminish the errors in estimation of the model parameters, the final fitting procedure was performed on the assumption that $K_{eb}(\infty) = K_{eb}(0)$ and f_r and n are constant.

Physical parameters of the model outnumber the independent fitting parameters. To solve this problem, in the determination of the model parameters it was assumed that $(\Delta\tilde{S}^{max}/S)\ [d] = 0.025 \pm 0.005$ and that $\overset{\#}{m}$ is independent of the type of the considered process. Results are presented in Tables 1 and 2 (see Results).

Electrofusion

It was assumed that the electrofusion yield, *efe*, is proportional to the increase in the energy of intermolecular interactions responsible for membrane integrity above the certain threshold value

$$efe = \frac{1}{2e[f]}\left[\gamma_{init}\frac{\Delta\tilde{S}^{max}}{S} + \alpha\chi\dot{q}^{e} - e_0[f]\right] \times 100\% \qquad (A26)$$

where $e_0[f]$ is threshold value of the increase in energy when electrofusion yield equals 0%, and $e[f]$ is the increase in energy relative to the threshold value when electrofusion yield equals 50%.

Additionally, it was assumed for simplicity that, within the experimental range of frequencies,

$$\gamma_{init}\frac{\Delta\tilde{S}^{max}}{S} \approx e_0[f]\alpha\chi\dot{q}^{e} \qquad (A27)$$

Thus Eqs. A26 and A27 led to

$$efe = \frac{1}{2e[f]}\alpha\chi^{e} \times 100\%. \qquad (A28)$$

On the basis of Equations A7, A15, and A28, the electrofusion yield was expressed as follows.

$$efe = \frac{1}{e[f]}\frac{\alpha\omega^2\eta_{eb}(2\omega)\chi(\sigma_0^e)^2}{[K_{eb}(2\omega) - 4\overset{\#}{m}\omega^2]^2 + [2\omega\eta_{eb}(2\omega)]^2} \times 100\% \qquad (A29)$$

Theoretical predictions (Eqs. A16, A17, and A29) were fitted to the published experimental results (6). (Fig. 8). In the calculations field strength was accepted to be $E_0 = 3.5 \times 10^5$ (V/m); the remaining parameters were taken from Appendix 2. Within the investigated range of field frequencies, the preliminary computer simulations suggested an insignificant contribution of the variations of the elasticity and viscosity of the erythrocyte membrane. Errors in estimation of the model parameters were reduced upon assumption of $K_{eb}(\infty) = K_{eb}(0)$ and $\eta_{eb}(\infty) = \eta_{eb}(0)$ for the final fitting procedure. Physical parameters were estimated on three additional assumptions: $K_{eb}(0) = (4.5 \pm 1.4) \times 10^7$ (N/m^2), $\alpha = 1/100$ (as reported under Discussion for *N. crassa* or Tib9) and $\chi = 3 \times 10^{-4}$ (s). The value of parameter χ represents the time of electric field application. The results are presented in Table 3 (see Results).

APPENDIX 2

Electric and geometric parameters used in the calculations are listed in the following table (Table A1).

	N. crassa	Tib9	RBC	Units
$Re[\dot{\epsilon}]/\epsilon_0$	45	45	60	
$Re[\dot{\hat{\epsilon}}]/\epsilon_0$	7.9	9.4	1.5	
$Re[\dot{\check{\epsilon}}]/\epsilon_0$	80	80	80	
$Im[\dot{\epsilon}]/\epsilon_0$	0	0	0	
$Im[\dot{\hat{\epsilon}}]/\epsilon_0$	0	0	0	
$Im[\dot{\check{\epsilon}}]/\epsilon_0$	0	0	0	
$Re[\dot{k}]$	0.229	0.1	0.5	S/m
$Re[\dot{\hat{k}}]$	0	0	0	S/m
$Re[\dot{\check{k}}]$	0.012*	0.002*	0.02	S/m
$Im[\dot{k}]$	0	0	0	S/m
$Im[\dot{\hat{k}}]$	0	0	0	S/m
$Im[\dot{\check{k}}]$	0	0	0	S/m
R	15×10^{-6}‡	6.5×10^{-6}	4×10^{-6}	m
d	9×10^{-9}	9×10^{-9}	9×10^{-9}	m
ϵ_0		8.8542×10^{-12}		F/m

* Accepted in calculations illustrated in Fig. 1.
‡ In the calculations illustrated in Fig. 1 *a*, R was obtained for each individual cell.

The experiments with Tib9 cells were performed at the Department of Biochemistry, University of Minnesota, by one of us (P. Marszałek). We are greatly indebted to Professor T. Y. Tsong for his help and stimulating discussions and to Carol Gross for editorial suggestions.
A part of this work is a fragment of the MS thesis of I. Szutowicz, presented at the Warsaw University, 1992. We are indebted to Dr J. J. Zieliński for valuable discussions. We thank Teresa Rak for cultures of *N. crassa* cells.

REFERENCES

1. Pawłowski, P., and M. Fikus. 1993. Bioelectrorheological model of the cell. 4. Analysis of the extensil deformation of the membrane in an alternating electric field. *Biophys. J.* 65:535–540.
2. Fikus, M., E. Grzesiuk, P. Marszałek, S. Różycki, and J. Zieliński. 1985. Electrofusion of *N. crassa* slime cells. *FEMS Microbiol. Lett.* 27:123–127.
3. Fikus, M., P. Marszałek, S. Różycki, and J. Zieliński. 1987. Dielectrophoresis and electrofusion of *Neurospora crassa* slime. *Studia Biophys.* 119:73–76.
4. Marszałek, P., D.-S. Liu, and T. Y. Tsong. 1990. Schwann equation and transmembrane potential induced by alternating electric field. *Biophys. J.* 58:1053–1058.
5. Warncke, J., and C. L. Slayman. 1980. Metabolic modulation of stoichiometry in a proton pump. *Biochim. Biophys. Acta.* 591:224–233.
6. Chang, D. C. 1989. Cell poration and cell fusion using an oscillating electric field. *Biophys. J.* 56:641–652.
7. Poznański, J., P. Pawłowski, and M. Fikus. 1992. Bioelectrorheological model of the cell. 3. Viscoelastic shear deformation of the membrane. *Biophys. J.* 61:612–620.
8. Needham, D., and R. M. Hochmuth. 1989. Electro-mechanical permeabilization of lipid vesicles. Role of membrane tension and compressibility. *Biophys. J.* 55:1001–1009.
9. Wolfe, J., and P. L. Steponkus. 1983. Mechanical properties of the plasma membrane of isolated plant protoplasts. Mechanism of hyperosmotic and extracellular freezing injury. *Plant Physiol.* 71:276–285.
10. Evans, E. A., and R. M. Hochmuth. 1978. Mechanochemical properties of membranes. *In* Current Topics in Membranes and Transport. F. Bronner and A. Kleinzeller, editors. Academic Press, New York, San Francisco, London. Vol. 10, 1–64.
11. Pawłowski, P., and M. Fikus. 1989. Bioelectrorheological model of the cell. 1. Analysis of stresses and deformations. *J. Theor. Biol.* 137:321–337.
12. Fikus, M., and P. Pawłowski. 1989. Bioelectrorheological model of the cell. 2. Analysis of creep and its experimental verification. *J. Theor. Biol.* 137:365–373.